International Journal of Fluid Mechanics & Thermal Sciences
2023; 9(2): 20-28
http://www.sciencepublishinggroup.com/j/ijfmts
doi: 10.11648/j.ijfmts.20230902.11
ISSN: 2469-8105 (Print); ISSN: 2469-8113 (Online)

Simulating Mixed Convection in a Lid-Driven Wavy Enclosure with Block in Different Locations

Sree Pradip Kumer Sarker[1, *], Mohammad Mahmud Alam[1], Mohammod Jahirul Haque Munshi[2]

[1]Department of Mathematics, Dhaka University of Engineering and Technology (DUET), Gazipur, Bangladesh

[2]Department of Mathematics, Hamdard University Bangladesh, Munshigonj, Bangladesh

Email address:

pradip.duet@gmail.com (Sree Pradip Kumer Sarker), alamdr.mahmud@duet.ac.bd (Mohammad Mahmud Alam), drmunshi@hamdarduniversity.edu.bd (Mohammod Jahirul Haque Munshi)

[*]Corresponding author

To cite this article:

Sree Pradip Kumer Sarker, Mohammad Mahmud Alam, Mohammod Jahirul Haque Munshi. (2023). Simulating Mixed Convection in a Lid-Driven Wavy Enclosure with Block in Different Locations. *International Journal of Fluid Mechanics & Thermal Sciences*, *9*(2), 20-28. https://doi.org/10.11648/j.ijfmts.20230902.11

Received: November 17, 2023; **Accepted**: December 4, 2023; **Published**: December 11, 2023

Abstract: Mixed convection in a wavy enclosure driven by a lid and including rectangular shaped blocks at various positions is the focus of this paper's simulation investigation. In this investigation, we also looked at how the heat transfer enhancement changed depending on the orientation of the heated block in relation to the stream. The control equations for mass, thermal energy, and Navier-Stokes are solved numerically using the Galerkin weighted residual finite element method. The enclosure contains two rectangular shaped heated blocks strategically positioned at varying heights - one set closer to the lower section of the enclosure, another situated at the mid-section of the enclosure and final set closer to upper wavy surface. The thermal insulation property of the wavy top wall, coupled with active heating of the bottom wall and blocks, creates a dynamic convective environment. Also, the lid-generated flow is driven by the left wall moving upwards and the right wall moving downwards. Richardson number impacts on streamlines, isotherms, dimensionless temperature, velocity profiles, average Nusselt numbers, and other characteristics are investigated in this study. Visualizations of these impacts are made possible using graphics. Inside the container, two eddies spun counterclockwise in every instance. Regardless of other factors, a higher rotating speed yields better performance. Enhanced heat transport would also be the outcome of a well-balanced set of regulating factors.

Keywords: Mixed Convection, Lid-Driven, Wavy Top, FEM and Heated Blocks

1. Introduction

The interplay of natural and forced convection in enclosed geometries is a critical phenomenon with broad implications in engineering and industrial processes. One particular configuration that has garnered attention is the lid-driven enclosure, characterized by its dynamic flow patterns induced by the motion of bounding walls. Understanding and optimizing heat transfer in such enclosures is paramount for applications ranging from electronics cooling to energy conversion systems. This study delves into the intricacies of mixed convection within a lid-driven enclosure distinguished by a wavy-shaped top surface. The unique undulating geometry of the upper boundary amplifies the complexity of the convective flow. Adding to this complexity, two heated rectangular-shaped blocks are strategically positioned within the enclosure. These blocks are situated in three distinct arrangements: bottom, middle and top of the enclosure. This strategic placement is anticipated to impart distinct thermal and flow characteristics to the system.

The top wavy wall is designated as a thermal insulator, emphasizing the dominant role of the bottom wall and heated blocks in driving the convective flow. Additionally, to further augment the forced convection, the left wall is programmed to move upwards, while the right wall moves downwards. This orchestrated motion of the bounding walls establishes a lid-driven flow, superimposing an additional layer of complexity on the convective heat transfer. The exploration of mixed convection within confined geometries has been a

subject of significant research interest, driven by its relevance in diverse engineering applications. A selection of key studies in this domain is discussed below:

Azizul et al. [1] provided insights into the complex heat transfer patterns of mixed convection by visualizing heat lines in a hollow driven by two lids and including a heated wavy wall. The work of Jani et al. [2] is significant because it delves into the topic of magnetohydrodynamic free convection in a square cavity heated from below, which sheds light on the relationship between convective heat transport and magnetic fields. In order to better understand the intricate flow dynamics that occur in right triangle enclosures, Ching et al. [3] used finite element simulations to investigate mixed convection heat and mass transfer. To further understand how magnetic fields affect heat transfer properties, Hossain et al. [4] performed a finite element analysis on mixed-mode free convection flow in a heated circular cylinder housed in an open square cavity. Using a multigrid technique, Kumar et al. [5] investigated flow and heat transfer behaviors in non-Darcy models for mixed convection in a porous cavity. The authors Senthil Kumar et al. [6] used numerical simulations with a velocity-vorticity formulation to study the effects of vorticity and velocity fields on double diffusive mixed convection in a square cavity controlled by a lid. Contributing to our understanding of flow patterns and temperature distributions in such designs, Rahman et al. [7] investigated mixed convection flow in a rectangular vented cavity with a heat-conducting square cylinder at its center. Mahjabin and Alim [8] gathered useful information about the influence of magnetic fields by studying the free convective flow of MHD fluid in a square cavity with a heated cone of variable orientation and how the Hartmann number affected it. To better understand the interplay between magnetic and thermal impacts on flow patterns, Chamkha [9] studied hydro-magnetic combined convection flow in a vertical lid-driven hollow with internal heat generation or absorption. To further understand the complexities of convective heat transfer in such enclosures, Prasad and Koseff [10] investigated the combined forced and natural convection heat transfer in a deep lid-driven hollow flow. Munshi et al. [11] explored the numerical modeling of nanofluid mixed convection heat transfer in a square enclosure with a lid-driven porous medium. Hydrodynamic mixed convection in a lid-driven square cavity is the subject of another study by Munshi [12]. This particular study incorporates an elliptically shaped heated block with a corner heater. Using a lid-driven porous square cavity with an interior elliptically shaped adiabatic block and linearly side walls, Munshi et al. [13] examined the optimization of mixed convection. In a wavy-top enclosure with a semicircular heater, Islam et al. [14] analyzed the simulation of natural convection flow using Magneto-Hydrodynamics. In addition, Munshi et al. [15] simulated hydrodynamic mixed convection in a hexagonal chamber with a heater at each corner using numerical methods. These studies collectively form a comprehensive body of research that encompasses various aspects of mixed convection in confined geometries, providing a solid foundation for the present investigation. The numerical methodologies employed in these studies, including finite element methods [16, 17], have proven to be invaluable tools for simulating and understanding complex convective flows.

Here is the structure of the sections that follow: The second section presents the geometrical arrangement. To explain the issue, the theoretical framework is laid out in Section third. The solution strategy is covered in Section fourth. In section fifth, we can see the program validations. Section sixth presents the results of the numerical simulations. This section presents quantitative data and phenomenological patterns of fluid flow, excluding problems with consistency and convergence. There is a conclusion at the end of the document.

2. Geometrical Configuration

The study investigates the phenomenon of mixed convection within a specially designed enclosure characterized by distinct geometrical features and thermal boundary conditions. The enclosure is defined in figure 1 by the following parameters:

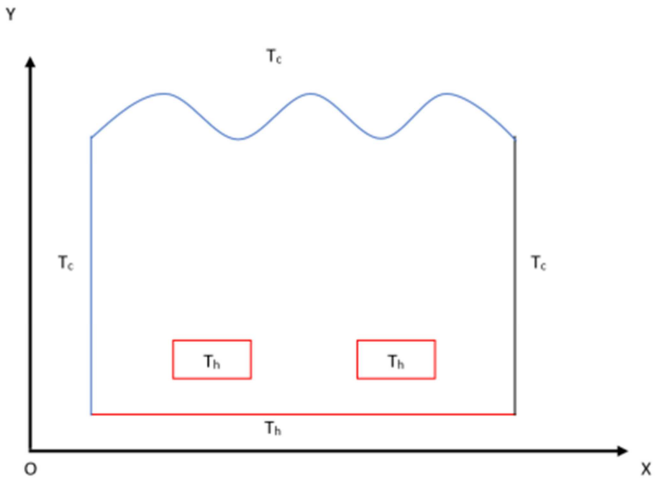

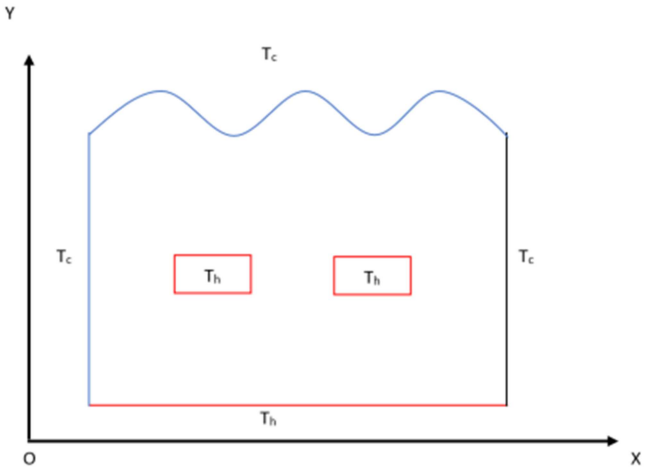

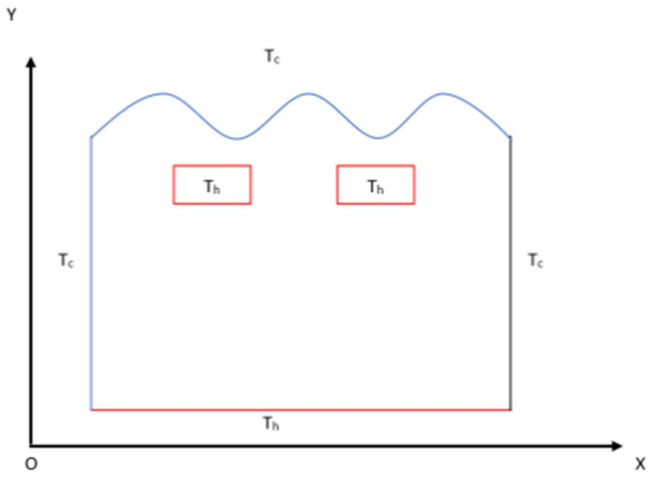

Figure 1. *Visual representation of the studied lid-driven wavy enclosure showing several blocks in various positions.*

The enclosure takes the form of a rectangular domain with defined length, width, and height dimensions. The top wall exhibits a distinctive wavy contour, imparting a non-uniform surface profile to the enclosure. This wall is thermally insulated, implying that it does not participate in the heat exchange process. The bottom wall of the enclosure is subjected to uniform heating, serving as one of the primary sources of thermal energy in the system. The left wall is configured to move in an upward direction, introducing an additional dynamic component to the system. It is also thermally insulated, meaning that it does not interact directly with the heat transfer process. In contrast to the left wall, the right wall moves in a downward direction, contributing to the dynamic behavior of the system. Similar to the left wall, the right wall is also thermally insulated. Two rectangular shaped blocks are positioned within the enclosure, and their placement varies for the three different scenarios under investigation. For the first scenario, the two rectangular shaped blocks are located nearer to the bottom of the enclosure. In the second scenario, the two rectangular shaped blocks are positioned nearer to the middle of the enclosure. And the third scenario, the two rectangular shaped blocks are positioned nearer to the top of the enclosure. Each of these blocks is subjected to uniform heating, acting as additional heat sources within the system.

3. Mathematical Formulation

The mathematical formulation for the study on mixed convection in the described enclosure involves the conservation equations for mass, momentum, energy, and the equations representing the boundary conditions. Given the complexity of the scenario, let's break down the key dimensional equations:

$$\frac{\partial \mathrm{u}}{\partial \mathrm{x}}+\frac{\partial \mathrm{v}}{\partial \mathrm{y}}=0$$

$$u\frac{\partial \mathrm{u}}{\partial \mathrm{x}}+\frac{\partial \mathrm{u}}{\partial \mathrm{y}}=-\frac{1\partial \mathrm{p}}{\rho \partial x}+v\left(\frac{\partial^2 u}{\partial x^2}+\frac{\partial^2 u}{\partial y^2}\right)$$

$$u\frac{\partial v}{\partial x}+v\frac{\partial v}{\partial y}=-\frac{1\partial p}{\rho\,\partial y}+v\left(\frac{\partial^2 v}{\partial x^2}+\frac{\partial^2 v}{\partial y^2}\right)+g\beta(T-T_c)$$

$$u\frac{\partial T}{\partial x}+v\frac{\partial T}{\partial y}=\alpha\left(\frac{\partial^2 T}{\partial x^2}+\frac{\partial^2 T}{\partial y^2}\right)+\frac{Q_0\left(T-T_c\right)}{\rho\, C_p}$$

Dimensional boundary conditions:

Top wavy wall: $u=v=0, T=T_c, 0\le x\le L,$

$$y=\frac{L}{2}(1+sin2n\pi x)$$

Bottom wall: $u=v=0, T=T_h, 0\le x\le L$

Left wall: $u=v=0, \frac{\partial T}{\partial x}=0, 0\le y\le \frac{L}{2}$

Right wall: $u=v=0, \frac{\partial T}{\partial x}=0, 0\le y\le \frac{L}{2}$

The equations are dimensional by using the following dimensionless parameters

$$X=\frac{x}{L}, Y=\frac{y}{L}, U=\frac{u}{U_0}, V=\frac{v}{U_0}, P=\frac{p}{\rho U_0^2}, \theta=\frac{T-T_c}{T_h-T_c}$$

$$Pr=\frac{\nu}{\alpha}, Re=\frac{VL}{\nu}, Gr=\frac{g\beta(T_h-T_c)L^3}{\nu^2}, Ri=\frac{Gr}{Re^2}, \nu=\frac{\mu}{\rho}$$

Here, X and Y are dimensionless coordinates varying along horizontal and vertical directions, respectively; U and V are dimensionless velocity components in the X and Y directions, respectively. θ is the dimensionless temperature, P is the dimensionless pressure, Q is the heat generation parameter; Re, Pr, Gr and Ri are Reynolds number, Prandtl's number and Grashof numbers and Richardson number respectively.

The dimensionless governing equations:

$$\frac{\partial U}{\partial x}+\frac{\partial V}{\partial Y}=0$$

$$U\frac{\partial U}{\partial x}+V\frac{\partial V}{\partial Y}=-\frac{\partial P}{\partial X}+\frac{1}{\mathrm{Re}}\left(\frac{\partial^2 U}{\partial X^2}+\frac{\partial^2 U}{\partial Y^2}\right)$$

$$U\frac{\partial U}{\partial x}+V\frac{\partial V}{\partial Y}=-\frac{\partial P}{\partial Y}+\frac{I}{\mathrm{Re}}\left(\frac{\partial^2 U}{\partial X^2}+\frac{\partial^2 U}{\partial Y^2}\right)+Ri\theta$$

$$U\frac{\partial \theta}{\partial x}+V\frac{\partial \theta}{\partial Y}=\frac{1}{\mathrm{Re}\,\mathrm{Pr}}\left(\frac{\partial^2 \theta}{\partial X^2}+\frac{\partial^2 \theta}{\partial Y^2}\right)+Q\theta$$

Dimensionless boundary conditions:
Top wavy wall: $= V = 0, \theta = 0$
Bottom wall: $U = V = 0, \theta = 1$
Left wall: $U = V = 0, \frac{\partial \theta}{\partial N} = 0$
Right wall: $U = V = 0, \frac{\partial \theta}{\partial N} = 0$

Richardson number is an important parameter to study the mixed convection phenomenon. where $Ri = 1$, it signifies the case as pure convection. If Richardson number is low $(Ri < 1)$ the viscous force dominates the flow, and the flow can be assumed to be assisted by forced convection. But when Richardson number has higher values $(Ri > 1)$ the buoyancy force dominates the viscous force, and the fluid flows as a result of natural convection. Osborne Reynolds in 1883, with the help of a simple experiment, demonstrated the existence of the following two types of follows. The Reynolds number $Re < 2000$ the flow is laminar and $Re > 4000$ the flow is turbulent. Reynolds number between 2000 and 4000 indicates a transition from laminar to turbulent flow.

The heat transfer coefficient in terms of local Nusselt number (Nu) is defined by,

$$Nu = -\frac{\partial \theta}{\partial \eta}$$

where η is the outward drawn normal on the plane.

Dimensionless normal temperature gradient can be written as

$$\frac{\partial \theta}{\partial \eta} = \sqrt{\left(\frac{\partial \theta}{\partial X}\right)^2 + \left(\frac{\partial \theta}{\partial Y}\right)^2}$$

While the average Nusselt number $\overline{Nu}$ is obtained by integrating the local Nusselt number along the bottom surface of wavy enclosure and is defined by

$$\bar{N}_u = -\frac{1}{L}\int_0^L \frac{\partial \theta}{\partial \eta} ds$$

Where θ is the dimensionless coordinate along the circular surface. If L=1for length of the enclosure then,

$$\bar{N}_u = -\int_0^L \frac{\partial \theta}{\partial \eta} ds$$

4. Numerical Technique

The dimensionless form of my physical problem is created from the dimensional governing equations. Using the Galerkin-Weighted Residual formulation and the finite element method [15], the governing equations and boundary conditions are solved numerically. The following standards are used to ensure that all dependent variables inside the solution domain meet the goal of convergence

$$\sum \left|\varphi_{i,j}^{n} - \varphi_{i,j}^{n-1}\right| \le 10^5$$

where φ represents the dependent variables *U, V, P* and *T* the indexes *i,j* refers to space coordinates and the index *n* is the current iteration.

5. Validation of a Program

Figure 2 illustrates the contrast between streamlines and isotherms for the graphical solution. The numbers clearly show that the two results coincide very well with one another.

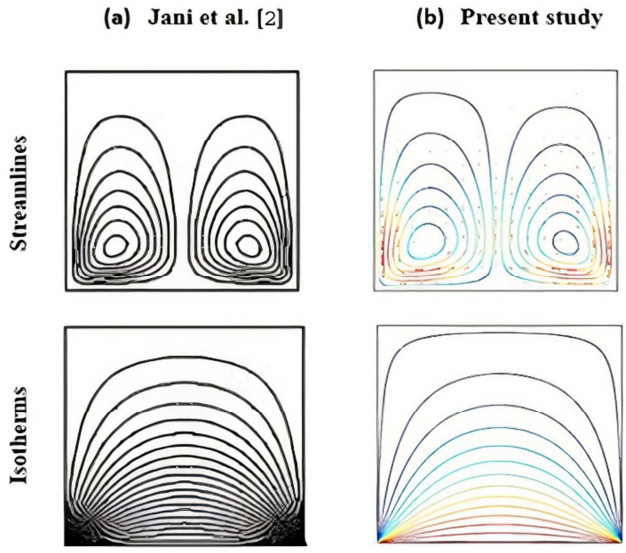

Figure 2. *Comparison between streamlines and isotherms for graphical solution of (a) Jani et al. [2] and (b) Present study at* $Ra = 10^4$ *and* $Ha = 50$..

6. Results and Discussions

Understanding the intricate flow and heat transfer properties of the system has been greatly enhanced by simulating mixed convection in a lid-driven wavy enclosure with blocks in varied places. The findings are applicable to the Richardson number in the range of 0.01 to 5. The findings are displayed using streamlines and isotherms within the various enclosing blocks. Figure 3 shows the variation of streamlines inside the enclosure with respect to the Richardson number, whereas Figure 4 shows the variation of isotherms. An extensive discussion follows the presentation of the following important findings.

The position of the heated blocks plays a critical role in

influencing the flow patterns and temperature distributions within the enclosure. Figure 3(a) where the blocks are positioned nearer the bottom position of the enclosure. As can be seen from the streamlines a pair of counter rotating eddies are formed in the enclosure. Also, localized upward flow along the wavy surface is observed. This phenomenon can be attributed to the combined effect of buoyancy-driven flow and the obstructing presence of the blocks. Conversely, in Figure 3(b), with the blocks nearer the middle of the enclosure, a more evenly distributed flow is noted. As can be seen from the streamlines in the Figure 3(c), a pair of counter rotating eddies are formed in the nearer the top position of the enclosure. From the streamlines it is found that with increasing the Richardson number the eyes of rotating eddies move up warded and close to the lid wall of the enclosure.

The wavy top wall acts as a thermal insulator, preventing heat transfer through conduction. This significantly affects the temperature distribution within the enclosure. The wavy geometry introduces additional complexities, resulting in the formation of distinct thermal boundary layers and recirculation zones. These features contribute to a non-uniform temperature profile, particularly in the vicinity of the wavy surface.

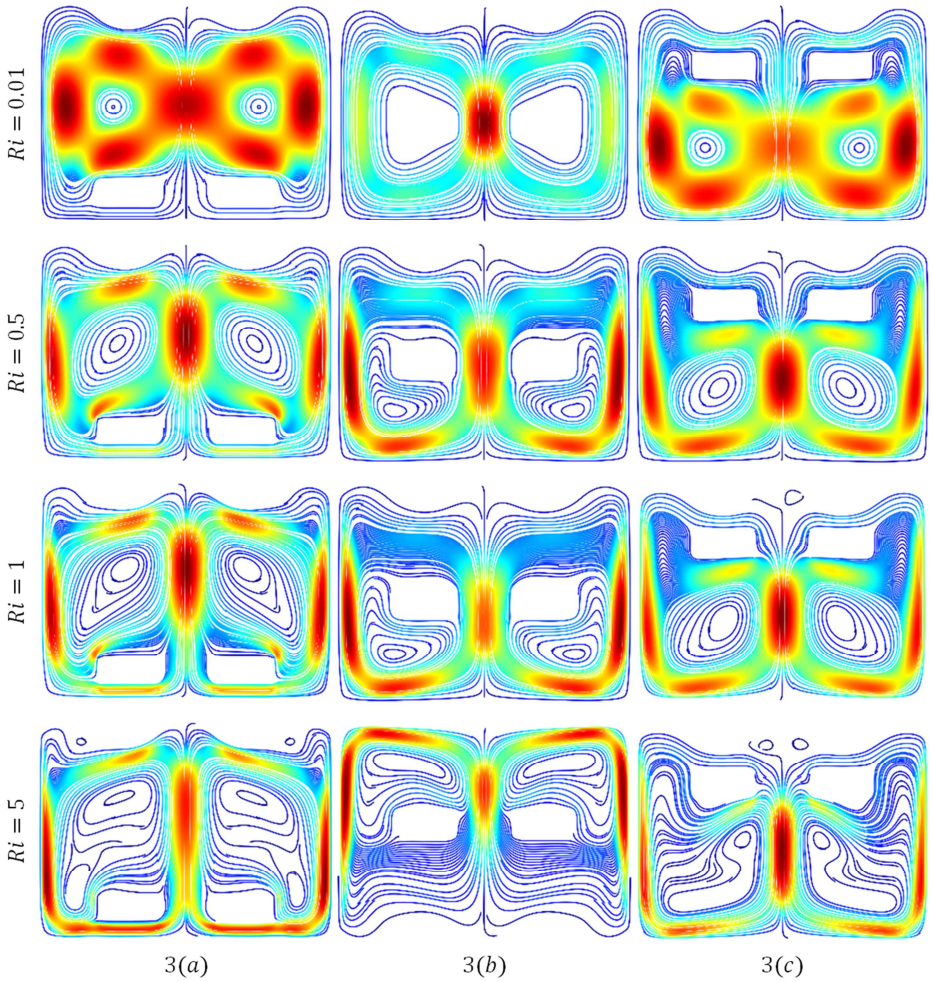

Figure 3. *Streamlines for different values of Richardson number with block in different locations while* $Pr = 0.71, Gr = 10^4$ *and* $Re = 100$.

Condition-dominated heat transfer is observed from the isotherms are shown in Figure 4. The isotherms lines appear parallel to the middle sides of the enclosure for the lowest value of Richardson number, indicating low heat transfer through convection are shown in Figure 4(a). In otherworld's, the isotherms lines near to the side walls for the different value of Richardson number and moving lid becomes strong, indicating low heat transfer through convection are shown if Figure 4(b) & 4(c). However, as the Richardson number increases, the isotherms bend more near the obstacle, indicating increased heat transfer through convection. These findings shed light on the complex interaction between the flow and heat transfer characteristics inside the enclosure, highlighting the important role of the Richardson number in controlling the heat transfer rate.

Figure 5 illustrates how the velocity components vary along a vertical line for different values of the Darcy number. The graph shows that as the Darcy number increases, both the maximum and minimum values of the velocity also increase. In other words, higher Darcy numbers lead to higher maximum and minimum velocities along the vertical line. This finding indicates that the Darcy number has a significant impact on the velocity distribution of the fluid.

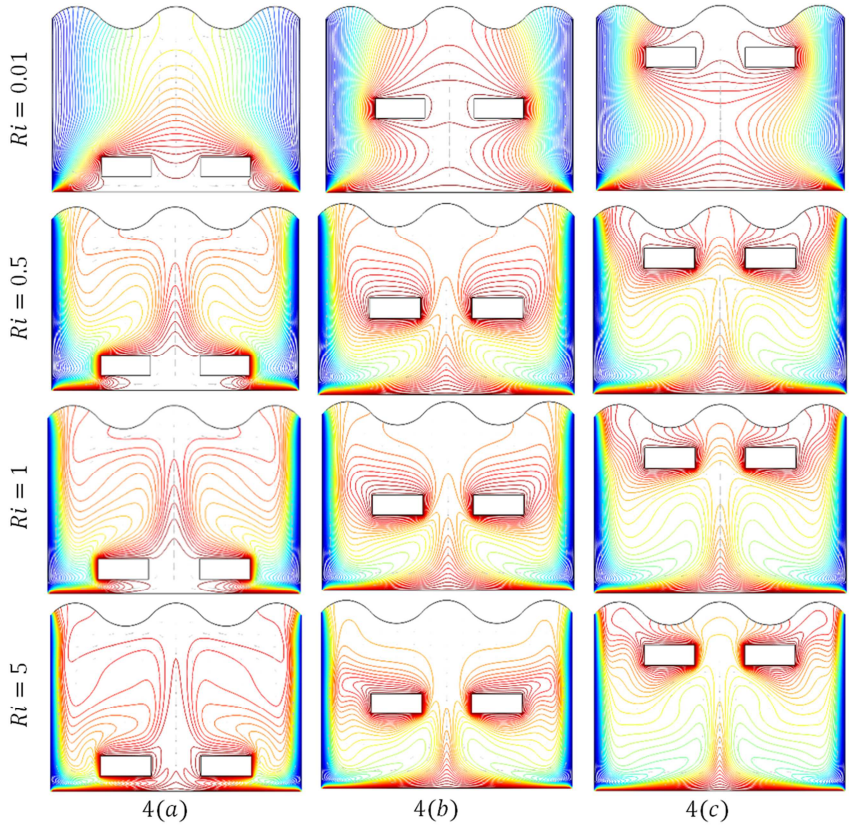

Figure 4. *Isotherms for different values of Richardson number with block in different locations while* $Pr = 0.71, Gr = 10^4 and\ Re = 100$.

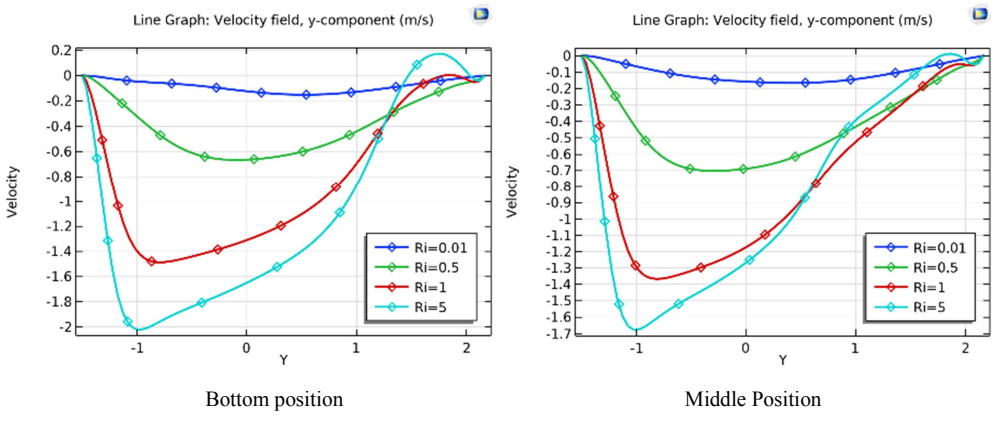

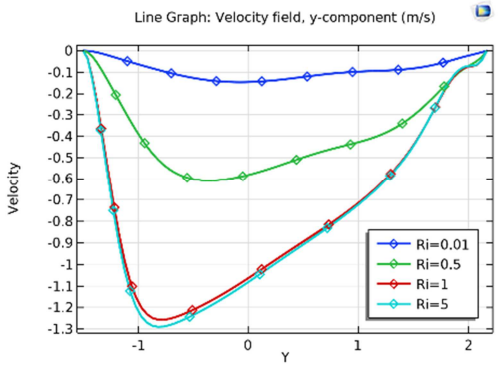

Figure 5. *Variation of velocity profiles along Y-axis for different values of Richardson number with block (a) Bottom position (b) Middle position and (c) Top position while* $Pr = 0.71, Gr = 10^4 and\ Re = 100$.

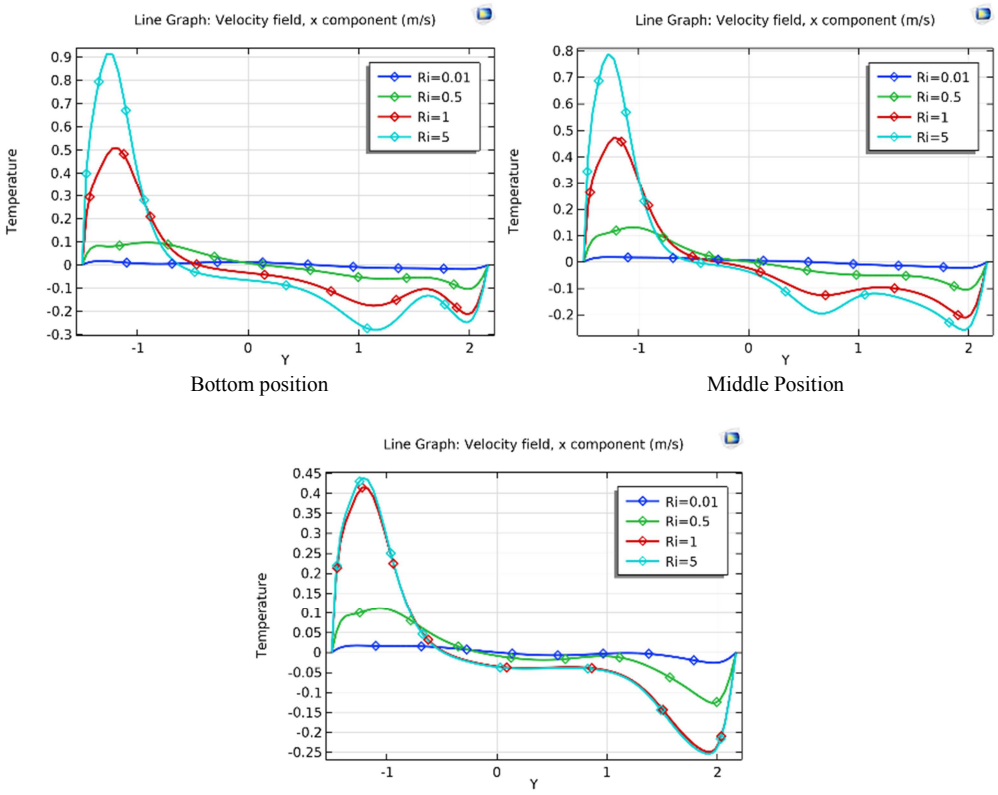

Figure 6. *Variation of dimensionless temperature along Y-axis for different values of Richardson number with block (a) Bottom position (b) Middle position and (c) Top position while* $Pr = 0.71, Gr = 10^4 and\ Re = 100$.

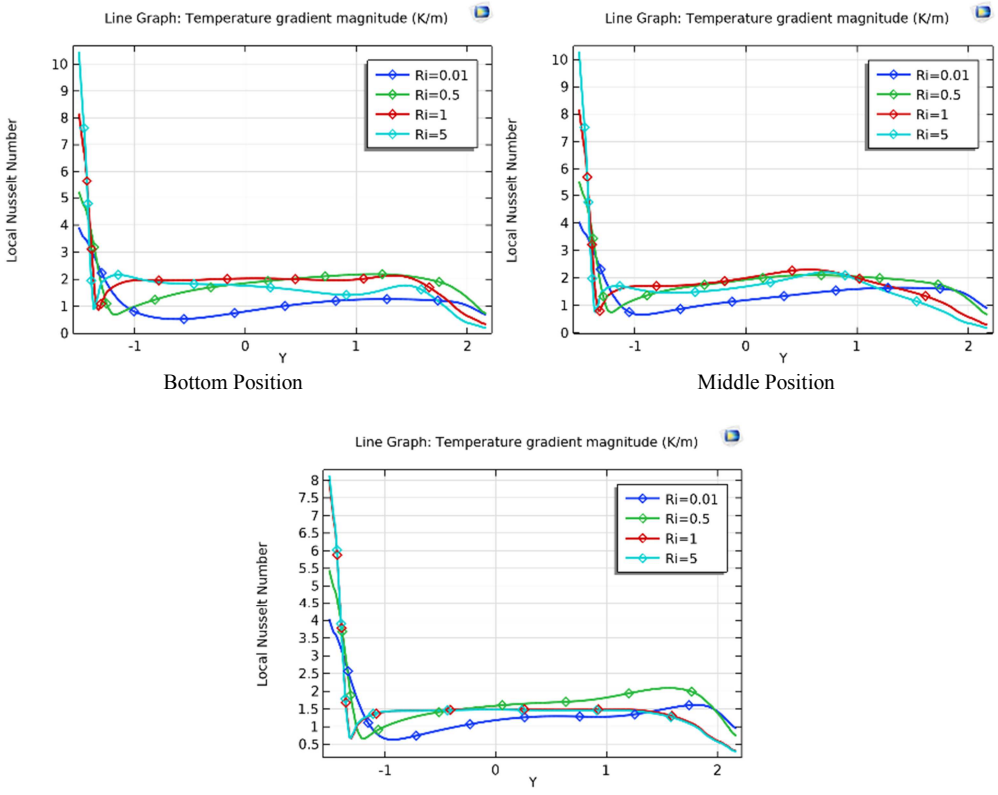

Figure 7. *Variation of local Nusselt number along Y-axis for different values of Richardson number with block (a) Bottom position (b) Middle position and (c) Top position while* $Pr = 0.71, Gr = 10^4 and\ Re = 100$.

Figure 5 shows how the enclosure's vertical velocity component varies for various Richardson numbers. The graphic clearly shows that when the Richardson number increases, the absolute values of the maximum and minimum velocities also increase. For various Richardson values, Figure 6 shows the Y-axis enclosure temperature variation with respect to the dimensionless temperature. The graph shows that the absolute values of the highest and lowest temperatures rise in direct proportion to the Richardson numbers. Worth mentioning, though, is that as the Richardson number increases, the temperature change rate decreases. Put simply, when the Richardson number is higher, the temperature variations along the Y-axis of the enclosure are slower. This result emphasizes how the Richardson numbers affect the liquid's temperature distribution and implies that a slower Y-axis temperature change is associated with greater Richardson numbers. Heat transfer grows in relation to both the buoyancy ratio and the Richardson numbers, as seen in Figure 7, which plots the local Nusselt number against various Richardson numbers. Why? Because it's at the stagnation point, where the fluid's velocity stops being a function of time and the heat transfer rate is at its highest. On the whole, the graph shows that many things affect the local Nusselt number, but that the stagnation point here at is where the heat transfer is at its highest.

7. Conclusion

This study investigated the intricacies of mixed convection within a lid-driven enclosure featuring a wavy top wall and heated rectangular shaped blocks positioned at varying heights. The enclosure was characterized by distinctive boundary conditions, including thermally insulating side walls, a heated bottom wall, and a top wall with a wavy contour. Additionally, the left wall exhibited an upward motion while the right wall moved in a downward direction, creating a unique flow environment.

The positioning of the heated blocks proved to be a crucial factor in determining the flow patterns and temperature distributions within the enclosure. When the blocks were located nearer to the top wavy enclosure, a localized upward flow along the wavy surface was observed. Conversely, positioning the blocks nearer the middle and bottom of the enclosure led to a more evenly distributed flow, resulting in a more uniform temperature distribution. The wavy top wall, acting as a thermal insulator, played a significant role in shaping the temperature profile within the cavity. The presence of the wavy geometry introduced complexities, leading to the formation of distinct thermal boundary layers and recirculation zones. The opposing motions of the side walls introduced additional vortical structures within the cavity, creating regions of high velocity gradients and turbulence. This further influenced both the flow patterns and the temperature distribution. Heating of the bottom wall and the blocks introduced buoyancy forces that drove the convective flow. The elevated temperature of the bottom wall generated an upward plume of warm fluid, influencing the overall flow patterns. Additionally, the presence of heated blocks induced local convection cells around them, resulting in localized variations in temperature and velocity.

Quantitative measures, such as Nusselt number, local heat transfer coefficients, and temperature gradients, were employed to characterize the heat transfer performance of the system. These metrics provided valuable data for evaluating the efficiency of the enclosure for specific applications.

In conclusion, this study sheds light on the intricate interplay of flow and heat transfer phenomena within the described enclosure configuration. The insights gained from this investigation provide a solid foundation for further studies aimed at optimizing the design of similar enclosures for a range of engineering applications. The findings presented herein contribute to the body of knowledge in the field of convective heat transfer and hold potential implications for the design of systems in various industrial and environmental contexts.

Conflicts of Interest

The authors declare no conflicts of interest.

References

[1] F. M. Azizul, A. I. Alsabry, I. Hashim, and A. J. Chamkha, "Heatline Visualization of Mixed Convection inside Double Lid-Driven Cavity having Heated Wavy Wall," Journal of Thermal Analysis and Calorimetry, vol. 145, pp. 3159-3176, 2020.

[2] S. Jani, M. Mahmoodi, and M. Amini, "Magnetohydrodynamic Free Convection in a Square Cavity Heated from Below and Cooled from Other Walls," International Journal of Mechanical, Aerospace, Industrial, Mechatronic and Manufacturing Engineering, vol. 7, pp. 750-755, 2013.

[3] Y. C. Ching, H. F. Öztop, M. M. Rahman, M. R. Islam, and A. Ahsan, "Finite Element Simulation of Mixed Convection Heat and Mass Transfer in a Right Triangular Enclosure," Int. J Heat Mass Transf., vol. 39, no. 5, pp. 689-696, May 2012.

[4] S. A. Hossain, M. A. Alim, and S. K. Saha, "A Finite Element Analysis on MHD Free Convection Flow in Open Square Cavity Containing Heated Circular Cylinder," American Journal of Computational Mathematics, vol. 5, pp. 41-54, 2015.

[5] D. S. Kumar, A. K. Dass, and A. Dewan, "Analysis of Non-Darcy Models for Mixed Convection in a Porous Cavity using a Multigrid Approach," Numer. Heat Transfer, vol. 56, no. 8, pp. 685-708, 2009.

[6] D. Senthil Kumar, K. Murugesan, and H. R. Thomas, "Numerical Simulation of Double Diffusive Mixed Convection in a Lid-Driven Square Cavity using Velocity-Vorticity Formulation," Numer. Heat Transfer A, vol. 54, no. 9, pp. 837-865, 2008.

[7] M. M. Rahman, M. Elias, and M. A. Alim, "Mixed Convection Flow in a Rectangular Ventilated Cavity with a Heat-Conducting Square Cylinder at the Center," Journal of Engineering and Applied Sciences, vol. 4, no. 5, pp. 20-29, 2009.

[8] S. Mahjabin and M. A. Alim, "Effect of Hartmann Number on Free Convective Flow of MHD Fluid in a Square Cavity with a Heated Cone of Different Orientation," American Journal of Computational Mathematics, vol. 8, pp. 314-325, 2018.

[9] A. J. Chamkha, "Hydromagnetic Combined Convection Flow in a Vertical Lid-Driven Cavity with Internal Heat Generation or Absorption," Numerical Heat Transfer, Part A, vol. 41, pp. 529-546, 2002.

[10] A. K. Prasad and J. R. Koseff, "Combined Forced and Natural Convection Heat Transfer in a Deep Lid-Driven Cavity Flow," International Journal of Heat and Fluid Flow, vol. 17, pp. 460-467, 1996.

[11] M. J. H. Munshi, M. A. Alim, A. H. Bhuiyan and K. F. U. Ahmed,"Numerical simulation of mixed convection heat transfers of nanofluid in a lid-driven porous medium square enclosure", American Institute of Physics (AIP), Vol. 2121, pp. 030005- (1-9), 2019.

[12] M. J. H. Munshi, M. A. Alim, A. H. Bhuiyan and M. Ali, "Hydrodynamic mixed convection in a lid-drivensquare cavity including elliptic shape heated block with corner heater", American Institute of Physics (AIP), Vol. 194, pp. 442- 449, 2017.

[13] M. J. H. Munshi, M. A. Alim, A. H. Bhuiyan, M. Ali,"Optimization of Mixed convection in a lid-driven porous square cavity with internal elliptic shape adiabatic block and linearly heated side walls", American Institute of Physics (AIP), 1851, 020049; doi: 10.1063/1.4984678, 2017.

[14] M. M. Islam, M. A. Alim, M. M. Alam, M. J. H. Munshi, "Simulation of Natural Convection flow with Magneto-Hytrodynamics in a wavy top enclosure with a semi-Circular heater", Open Journal of Applied Sciences, Scientific Research Publicising, Vol. 13, pp. 591-603, 2023.

[15] M. J. H. Munshi, G. Mostafa, A, B. S, M. Munshi., M. Waliullah, " Hydrodynamic Mixed Convection in a Lid-driven hexagonal cavity with corner heater", American Journal of Computational Mathematics, Scientific Research Publicising, Vol. 8, No. 245- 258, 2018.

[16] J. N. Reddy, "An Introduction to Finite Element Method," McGraw-Hill, New York, 1993.

[17] O. C. Zienkiewicz and R. L. Taylor, "The finite element method," Fourth Ed., McGraw-Hill, 1991.